

Assessment of Nitro-Substituted Aminostilbene as Organic Sensitizer for Dye-Sensitized Solar Cell (DSSC) Application

Wan M. Khairul^{1*}, Rafizah Rahamathullah^{1,2}, Adibah Izzati Daud^{1,2},
Muhamad Yuzaini Azrai Mat Yunin¹

¹Advanced Nano Materials (ANoMa) Research Group, Faculty of Science and Marine Environment,
Universiti Malaysia Terengganu, 21030 Kuala Nerus, Terengganu, Malaysia

²Faculty of Engineering Technology, Universiti Malaysia Perlis, Sungai Chuchuh,
02100 Padang Besar, Perlis, Malaysia

*Corresponding author (e-mail: wmkhairul@umt.edu.my)

The research involving metal-free organic sensitizers owes intensive attention to their promising advantage of having electronic properties which arise from the designed molecules. Within this interest, nitro-substituted aminostilbene dye involving Donor (D)- π -Acceptor (A) concept has been integrated as organic sensitizer in dye-sensitized solar cell (DSSC) application. The synthesized compound was characterized for its physico-chemical assessment namely through infrared (IR), ultraviolet-visible (UV-Vis) and ¹H and ¹³C nuclear magnetic resonance (NMR) spectroscopy, thermal analysis and optical band gap (E_g^{opt}) that exhibited 2.61 eV, which lies within semiconductor properties. Further, theoretical evaluation on vibrational analysis, electronic transition and FMO analysis were calculated via density functional theory (DFT) and time-dependent DFT at B3LYP/6-31G (d, p) level basis set which gave comparable results with the experimental approach. The HOMO-LUMO gap of the dye exhibited 3.06 eV which should promise strong support of being a potential sensitizer candidate for optoelectronic application. The DSSC was fabricated using this dye under simulated solar radiation (100 mW cm⁻²) and achieved 0.0018% conversion efficiency.

Key words: Aminostilbene, spectroscopic, sensitizer, FMO level

Received: May 2019; Accepted: September 2019

In recent years, a new generation of organic dyes have been explored and developed in the hope to overcome main drawbacks of ruthenium complex sensitizers in terms of their limited availability, require an inert condition for synthetic workup and high cost of ruthenium metal [1-3]. Lately, researchers' interest towards the development of metal-free organic dyes as an alternative to transition metal complexes have increased significantly due to the advantages offered by organic dyes. Organic dyes are known to exhibit diverse and tuneable molecular structures, possess hyperchromic in molar extinction coefficients, ease of synthesis work-up, low cost of raw materials and environmentally friendly approach [4-6]. Most of the reported organic dyes based on conjugated molecules consist of three main parts, namely, an electron donating group, π -bridge and an electron withdrawing group (D- π -A). In this context, an intense research focusing on the alteration of systematically on push-pull effect features in order to achieve higher power conversion efficiencies. Indeed, the structure of coplanarity enables subsequent electron transfer to semiconductor and improves DSSCs-architecture performances. Additionally, the presence of stilbene acts as π -linker which can enhance the structural or spatial dimensions of π -conjugated molecules in order

to tune and attain more constructive physical properties [7-8]. In fact, despite of being widely used in biological and medicinal applications, stilbene derivatives also exhibit interesting features on absorbing light [9], optical brighteners [10] and as electroluminescent behaviour to investigate the conductivity and molecular properties in organic electronic application (i.e. DSSC). Particularly, tuning the photochemical and photophysical characteristics of stilbenes can be done through the incorporation of functional groups into a stilbene backbone.

Therefore, herein, we report the synthesis of nitro-substituted aminostilbene to be applied as organic sensitizer in DSSC, in which an electron-deficient nitro unit is connected to a donor group in D- π -A chromophores. This is due to the introduction of nitro to the molecular backbone which can lead to more red shift of absorption and emission bands. The presence of electron rich amino unit is achieved to be connected to an acceptor group in order to destabilize the energy of the highest occupied molecular orbital (HOMO) in D- π -A chromophore, leading to a red-shifted of emission band. This study involved a combination of theoretical modelling via Gaussian 09 software for density functional theory (DFT)

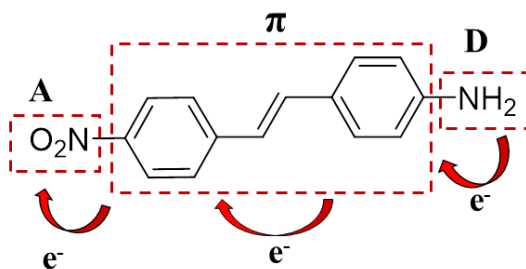


Figure 1. Molecular framework of 4-amino-4'-nitrostilbene derivative.

calculations in term of vibrational analysis, HOMO-LUMO energy gap and also the prediction of molecular conductivity. This synthesised nitro-substituted aminostilbene exhibited significant performances in providing ideal and rather good power conversion efficiency. Figure 1 illustrates the molecular framework of interest bearing nitro-substituted aminostilbene derivative.

EXPERIMENTAL SECTION

Materials

All chemicals, solvents and reagents were purchased from standard commercial suppliers, namely, Merck, Fisher Scientific, Across Organic, Sigma Aldrich and R&M Chemical, and were used as received without further purification during the synthesis workup. In this work, the chemicals and solvents used were 4-vinylaniline, 1-iodo-4-nitrobenzene, palladium(II) chloride, triphenylphosphine, dichloromethane, ethyl acetate, triethylamine, dimethylformamide, acetone, chloroform, hexane, acetonitrile and triethylamine. For the fabrication of photoanode and counter electrode of DSSCs, fluorine tin oxide (FTO) with sheet resistance 7 Ω /sq, chloroplatinic acid, TiO₂ paste (DSL 18NR-AO, Dyesol) and isopropanol were supplied by Sigma Aldrich.

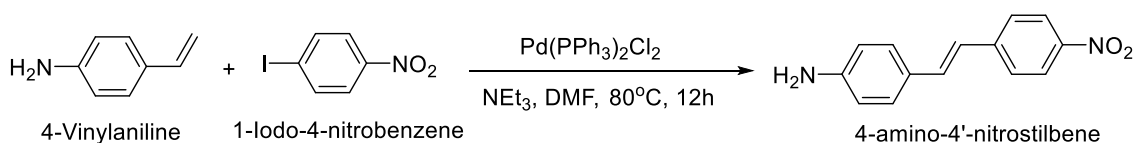
Instrumentation

Fourier-Transform Infrared (FT-IR) spectra were recorded on Perkin Elmer 100 FT-IR Spectroscopy using potassium bromide (KBr) pellets within the spectral range of 4000-450 cm^{-1} . The Nuclear Magnetic Resonance (NMR) spectra were recorded on Bruker Avance III 400 Spectrometer for ¹H (400.11 MHz) and ¹³C (100.61 MHz) by using deuterated chloroform (CDCl₃) as solvent, in ranges δ_{H} 0-15 ppm (¹H) and δ_{C} 0-200 ppm (¹³C), with trimethylsilane (TMS) as internal standard. For electronic transition analysis, UV-Visible spectroscopy analysis was

performed by using Shimadzu UV-Vis in 1 cm^3 cuvette within the range of λ_{max} 230-400 nm in 1×10^{-5} M dichloromethane (DCM). Thermogravimetric analysis was carried out using Perkin-Elmer TGA analyzer from 30°C to 900°C at a heating rate of 10°C/min under consistent nitrogen flow. The synthesized dye was deposited on photoanode ITO substrate and the current-voltage (*I-V*) characteristics were measured using electrochemical impedance spectroscopy (EIS) driven by Nova 1.10.1.9 software under illumination power of 100mW/cm² by AM 1.5 solar simulator.

Synthesis of 4-amino-4'-nitrostilbene

The workup with respect to the synthesis of 4-amino-4'-nitrostilbene have previously been reported in literatures [11-12]. However, some modifications in the preparation and additional characterization on the spectroscopic and analytical tasks have been carried out, improved and were discussed thoroughly in this report. The preparation of 4-amino-4'-nitrostilbene was proceeded via Heck cross-coupling reaction using a mixture of 4-vinylaniline (1.0 molar equivalence) and 1-iodo-4-nitrobenzene (1.5 molar equivalence), with Pd(PPh₃)₂Cl₂ as catalyst. The reaction was performed using triethylamine (NEt₃) and dimethylformamide (DMF) as base and solvent respectively, under reflux with constant stirring and aerobic condition. After adjudged completion by thin layer chromatography (TLC), the solution was cooled to room temperature prior to extraction of the organic layer. The organic layer was separated, dried over MgSO₄ and the solvent was removed *in-vacuo*. The residue obtained was then purified by using column chromatography and the collected sample after separation was then taken to dryness under reduced pressure to obtain brick-red solid of titled compound (0.58 g, 60%). The synthesis pathway of the preparation of 4-amino-4'-nitrostilbene is shown in Scheme 1.



Scheme 1. The preparation of 4-amino-4'-nitrostilbene.

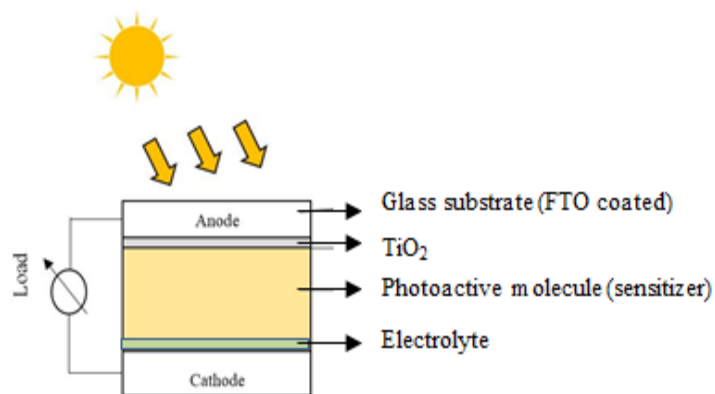


Figure 2. Schematic diagram of architectural design of DSSC.

Dye preparation and Fabrication of solid-state DSSC

The DSSC fabrication followed the previously reported method in the literature [13-15], by using the configuration glass/FTO/TiO₂/dye/electrolyte/Pt/FTO/glass. Nevertheless, slight modifications in terms of the dye and electrolyte were carried out and discussed in this report. Fluorine tin oxide (FTO) covered glass (2 cm × 2 cm) was used as the substrate in the fabrication of photoanodes. It was soaked in acetone and subsequently sonicated for about 10 min, followed by rinsing with isopropanol and deionized water. The TiO₂ paste was spread on clean FTO glass by using doctor blade technique and sintered at 450°C. Dye solutions were prepared using respective stilbene-

based compounds by dissolving in dichloromethane to prepare 0.01 M dye solutions. Accordingly, the TiO₂-based photoanodes were sensitized by soaking in the prepared dye solutions overnight. Then, the photoanodes were rinsed with ethanol to get rid of unabsorbed dye on the surface and dried at room temperature. The solid-state DSSC was assembled by sandwiching the sensitized photoanode and platinum-coated counter electrode with introducing solid polymer electrolyte (SPE) between the electrodes as depicted in Figure 2. This architectural layout is typical and common in any DSSC design involving this type of photoactive molecular system. The current-voltage (I-V) characteristics of DSSC were performed under solar illumination with incident light intensity of 100 mW/cm².

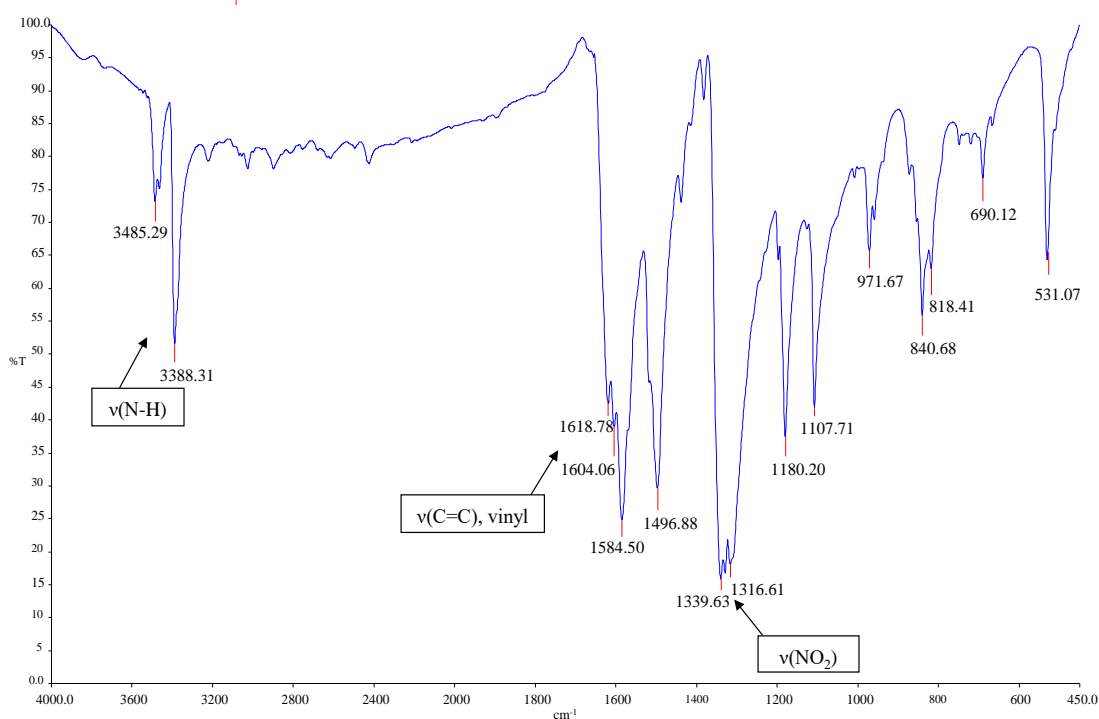


Figure 3. Infrared spectrum of 4-amino-4'-nitrostilbene.

Table 1. Experimental and theoretical vibrational frequencies of the compound and their respective assignments.

| Experimental IR (cm ⁻¹) | Theoretical IR (B3LYP / 6-31 G (d, p)) | | | |
|--|--|-----------|---------------------------------|----------------------------|
| | Freq (Scaled), cm ⁻¹ | Intensity | Unscaled freq, cm ⁻¹ | Vibrational assignments |
| 3485 | 3632 | 16.03 | 3695 | νN-H |
| 3388 | 3523 | 71.30 | 3584 | νN-H |
| 1604 | 1587 | 37.56 | 1614 | νC=C |
| 1496 | 1462 | 15.17 | 1487 | νC=C |
| 1340 | 1647 | 331.03 | 1660 | νN-O |
| 1585 | 1632 | 15.87 | 1676 | νN-O |
| 972 | 928 | 1.07 | 944 | bO-N-O |

v:stretching; *b*:in-plane bending

RESULTS AND DISCUSSION

Vibrational Analysis

The infrared spectroscopy of 4-amino-4'-nitrostilbene was recorded using Perkin Elmer 100 FTIR spectrophotometer within the spectral range 4000-450 cm⁻¹ as depicted in Figure 3. Whilst, the simulated FT-IR spectrum was carried out via Gaussian 09 of DFT (B3LYP) method using 6-31G (d, p) functional of theory. All the experimental and theoretical vibrational frequencies for the synthesised compound, along with the corresponding vibrational assignments are tabulated in Table 1. For the synthesised molecule of 4-amino-4'-nitrostilbene, there are three absorption bands of interest to be observed, namely, primary amine (NH₂), C=C and nitro substitution. The sharp absorption band at 1585 cm⁻¹ and the moderate band at 1340 cm⁻¹ represent the vibration of nitro (NO₂)

substitution and another weak band at 972 cm⁻¹ represents NO₂ bending [16-17], while the DFT calculation reveals this mode at 1598 cm⁻¹ and 1386 cm⁻¹ and 944 cm⁻¹ for NO₂ bending. The absorption of primary amine (NH₂) at higher wavenumbers exhibited two moderately intense N-H stretching frequencies corresponding to the asymmetrical and symmetrical N-H stretching vibrations. These bands were assigned at 3485 cm⁻¹ and 3388 cm⁻¹. Theoretically from DFT calculation, the N-H stretching of both asymmetrical and symmetrical can be observed at 3584 cm⁻¹ and 3695 cm⁻¹, respectively. Another important characteristic band shown by stilbene derivative is C=C stretching vibration, which can be clearly seen at between 1604 cm⁻¹ and 1498 cm⁻¹ in the FT-IR spectrum. Whilst, at 1614 cm⁻¹ and 1487 cm⁻¹ theoretically, at which the wavenumbers varied depending on the substituent groups attached to the stilbene molecular framework [18].

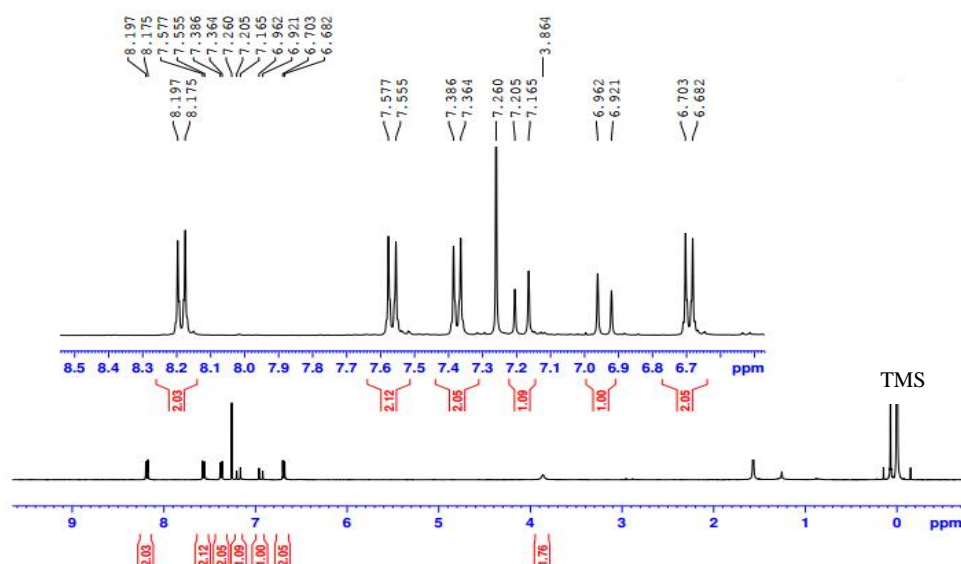


Figure 4. ¹H NMR spectrum of 4-amino-4'-nitrostilbene.

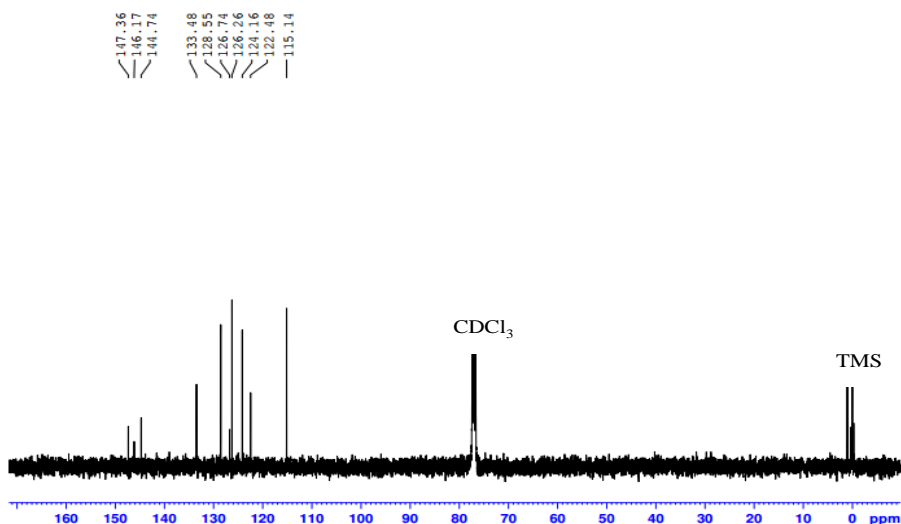


Figure 5. ^{13}C NMR spectrum of 4-amino-4'-nitrostilbene.

Nuclear Magnetic Resonance (NMR) Analysis

The ^1H NMR spectrum of 4-amino-4'-nitrostilbene (Figure 4) showed resonance of primary amine (NH_2) protons as weak and broad at δ_{H} 3.86 ppm. The aromatic protons could be detected within the range of δ_{H} 6.68-8.20 ppm as pseudo-doublet arising from the *para*-substituted aromatic ring of stilbene derivative. In this context, the presence of strong inductive electron-withdrawing effect of $-\text{NO}_2$ in the molecule decreased electron density around the resonances and shifted the protons to downfield position. The existence of two characteristics of doublet $\text{CH}=\text{CH}$ resonance observed at δ_{H} 6.96 ppm and δ_{H} 7.17 ppm with higher coupling constants ($J = 16$ Hz) indicated that ethylene moiety is in the *trans*-conformation [19-21]. In the ^{13}C NMR spectrum (Figure 5), the ethylene carbons were observed as two resonances at δ_{C} 126.74 ppm and δ_{C} 128.55 ppm, where the splitting is due to influence of its unsymmetrical structure. The aromatic carbon resonances can be observed within the range of δ_{C} 115.15-147.36 ppm, which is attributed to *para*-substituted aromatic ring.

Absorption Spectroscopy

The electronic absorption spectrum of 4-amino-4'-nitrostilbene as depicted in Figure 6 revealed two absorption bands which are expected to have arisen from phenyl ring, ethylene ($\text{C}=\text{C}$), amine (NH_2) and $-\text{NO}_2$ auxochrome. The strong intensity with broad absorption band can be seen at around λ_{max} 404 nm ($\epsilon=80,500 \text{ L mol}^{-1}\text{cm}^{-1}$), while the broad with weak absorption was detected at λ_{max} 290nm ($\epsilon=40,000 \text{ L mol}^{-1}\text{cm}^{-1}$), which is attributed from mixed transitions of $\pi\rightarrow\pi^*$ and $n\rightarrow\pi^*$. The $\pi\rightarrow\pi^*$ transition is mainly localized in the stilbene moiety and contributions from π -bonding orbitals of the aromatic ring, whereas $n\rightarrow\pi^*$ transition is ascribed to the amine (NH_2) chromophore. In these senses, the absorption of 4-amino-4'-nitrostilbene was shifted to bathochromic and hyperchromic shifts in which it was influenced by strong electron withdrawing group that has inductive effect interaction between the stilbene moiety and substitution strength on phenyl ring by $-\text{NO}_2$ auxochrome.

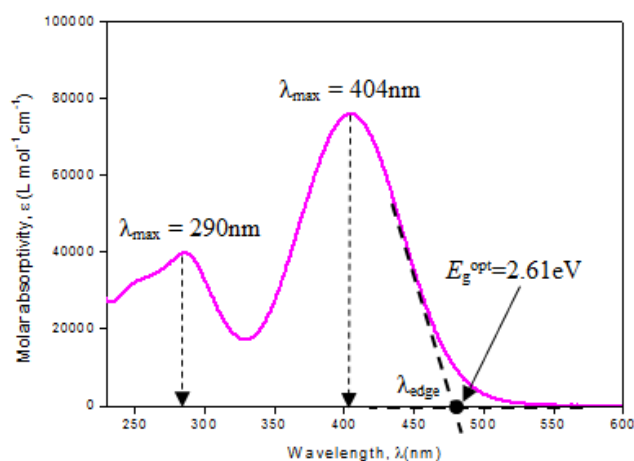


Figure 6. UV-Visible spectrum and optical gap of 4-amino-4'-nitrostilbene.

For further insight into optical properties of the stilbene-based compound, the optical band gap (E_g^{opt}) was measured using Eq. (1), where E_g^{opt} is expressed in eV and off-set is obtained from cut-off wavelength, which is the intercept of the linear portion of the UV-Vis spectrum expressed in nm [22-23].

$$E_g^{opt}(\text{eV}) = h \times \frac{c}{\lambda_{a.e}} \approx \frac{1240}{\lambda_{a.e.}(\text{nm})} \quad \text{Eq. (1)}$$

Here, h is Planck constant and c is speed of light in vacuum. Based on the UV-Vis spectrum, the cut-off wavelength (λ_{edge}) was found to be 475 nm which led to experimental optical energy band gap of 2.61 eV, as illustrated in Figure 6. In this sense, the obtained E_g^{opt} for 4-amino-4'-nitrostilbene is denoted in the typical band gap range for organic semiconducting materials, which indicates the suitability in acting as a potential candidate in optoelectronic application.

Quantum chemical calculation

The electronic transition and energy separation between highest occupied molecular orbital (HOMO) and lowest unoccupied molecular orbital (LUMO) of 4-amino-4'-nitrostilbene were carried out via TD-DFT B3LYP 6-31G (d,p) basis set and were computed. The combined and overlaid experimental and theoretical

prediction of UV-Vis spectra are illustrated in Figure 7. The values of wavelength (λ), oscillator strength (f), excitation energies (eV) and major contributors of electronic transitions are listed in Table 2.

The calculated absorption maxima of 4-amino-4'-nitrostilbene were notably slightly red shift (positive solvatochromism) compared to the experimental absorption. In this context, the calculated UV-Vis displayed similar trends with the experimental which revealed two bands at λ_{max} 425 nm (Exp. λ_{max} 404 nm) with oscillator strength ($f=0.7662$) and at around λ_{max} 304 nm (Exp. λ_{max} 290 nm) with oscillator strength ($f=0.4210$). Indeed, the transition peaks were attributed to mixed transitions of HOMO→LUMO ($n\rightarrow\pi^*$) and HOMO-1→LUMO ($\pi\rightarrow\pi^*$), which were comparable with the experimental data. For a clearer picture of the electronic properties, the frontier molecular orbitals (FMO) were computed and the main electronic transitions along with their respective $\Delta E_{HOMO-LUMO}$ energy values are represented in Figure 8. From the FMO analysis, we can clearly observe that HOMO and LUMO of 4-amino-4'-nitrostilbene are delocalized throughout the entire molecule including aromatic rings, *trans*-stilbene and NO₂ substitution group. In this sense, the HOMO-LUMO gap exhibits relatively small value, 3.06eV and falls in the range of semiconducting materials.

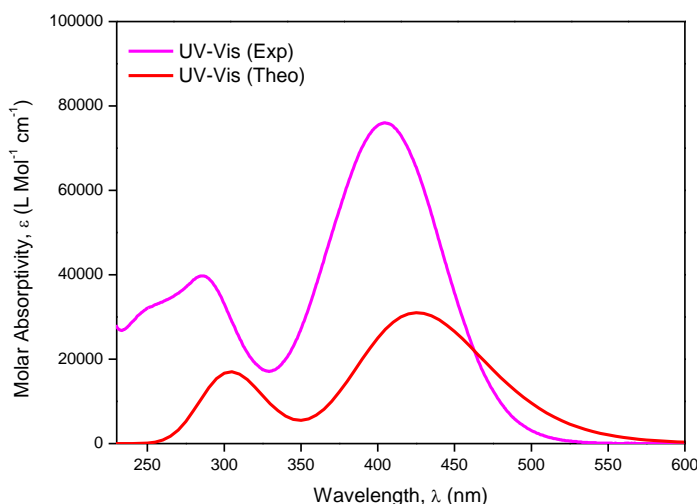


Figure 7. Experimental and computed UV-Vis spectra of 4-amino-4'-nitrostilbene.

Table 2. Excitation energy (ΔE), oscillator strength (f) and major contributors (%).

| Compound | Electronic transition | ΔE , eV | Wavelength (nm) | | Oscillator strength (f) | Major contributors (%) |
|---------------------------------|-----------------------|-----------------|-----------------|------------|-----------------------------|----------------------------|
| | | | Experimental | Calculated | | |
| 4-amino-4'-nitrostilbene | $S_0 \rightarrow S_1$ | 2.91 | 404 | 425 | 0.7662 | H→L (99%) |
| | $S_0 \rightarrow S_2$ | 4.07 | 290 | 304 | 0.4210 | H-1→L (14%) H→L+1 (74%) |

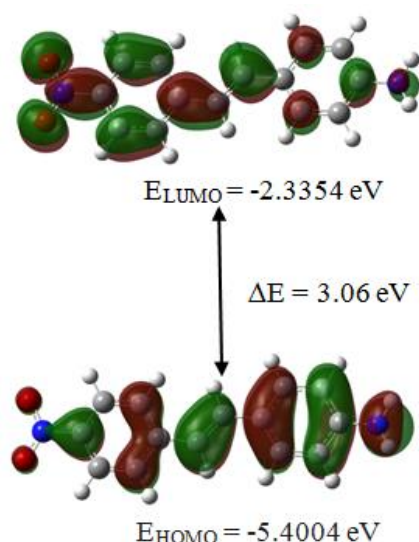


Figure 8. Frontier molecular orbital (FMO) for 4-amino-4'-nitrostilbene.

Thermal stability analysis

Thermal behaviour of 4-amino-4'-nitrostilbene exhibited good stability up to *ca.* 220°C and no weight loss occurred below 100 °C, which evidence there was no entrapped water molecule or solvent presence in the sample. The TGA/DTG curve revealed a single degradation step took place at around 220-225°C (T_{onset}) and ended at around 380-400°C (T_{offset}) with sharp endothermic DTG as illustrated in Figure 9. The higher remaining weight loss of 21.5% and char residue were produced at 900°C due to the presence of electronegative group, ethylene bond and left over of catalyst in the compound which need higher energy for bond cleavage and dissociate into smaller volatile fragments. During the decomposition of this stage, the total weight loss was about 78.5% with maximum degradation (T_{max}) occurred at 300°C. From the thermal behaviour analysis, the compound displayed thermal stability at high temperature and it gave good

indications to be applied in film fabrication as it exhibits remarkable performance under prolonged thermal stress.

Current-Voltage of DSSC performance

The performance of the fabricated DSSC was tested under illumination conditions of 100 mW/cm² via solar simulator to obtain I-V characteristics as illustrated in Figure 10. The corresponding photovoltaic parameters, namely open-circuit voltage (V_{oc}), short-circuit current density (J_{sc}), fill factor (FF) and solar conversion efficiency (η) under light intensity were computed in Figure 10 and the values are listed in Table 3. The efficiency was calculated using Eq. (2) where P_{in} is power incident ray intensity of 100 mW/m² and surface area cell of 4.0×10^{-4} m².

$$\eta (\%) = \frac{J_{sc} \cdot V_{oc} \cdot FF}{P_{in}} \quad \text{Eq. (2)}$$

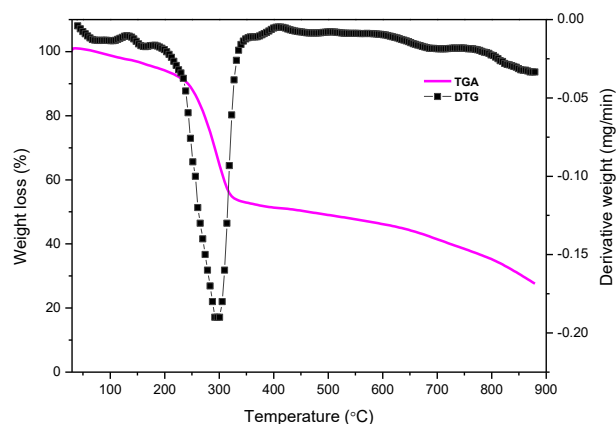


Figure 9. TGA/DTG thermogram of 4-amino-4'-nitrostilbene.

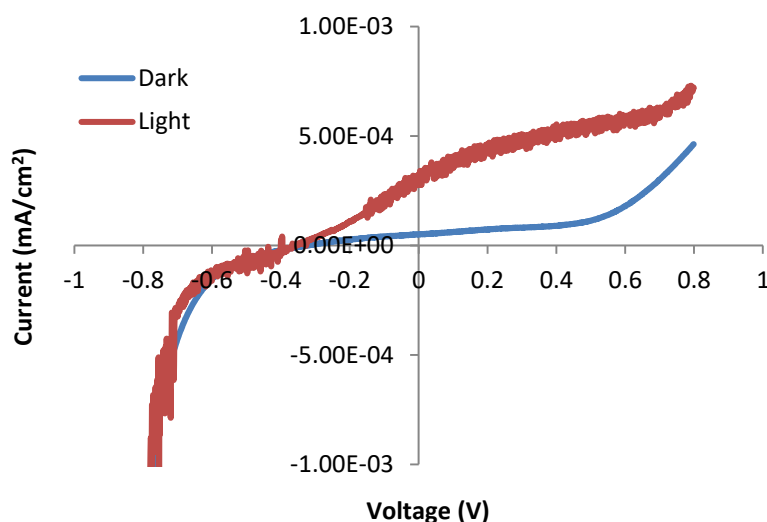


Figure 10. I-V curve of DSSC measurement.

Table 3. Summary of photovoltaic parameters of DSSC.

| Sample | V_{oc} (V) | J_{sc} (mA/cm ²) | Fill Factor | Efficiency (%) |
|---------------------------------|--------------|--------------------------------|-------------|----------------|
| 4-amino-4'-nitrostilbene | 0.4 | 3.08×10^{-4} | 0.59 | 0.0018 |

The photo-conversion efficiency (η) of DSSC fabricated using 4-amino-4'-nitrostilbene was found to be of lower value at only 0.0018%. This is due to the low performance of J_{sc} and poor contact at electrode-electrolyte interface which limit the transport of the redox couple components in the electrolyte and consequently affect the efficiency of the DSSC fabricated in this study [24]. Therefore, further investigation on designing fabrication architecture including modification of electrode and electrolyte should be carried out in order to ensure high collection of photocurrent and enhance conversion efficiency energy.

CONCLUSION

The role and performance of 4-amino-4'-nitrostilbene dye has been successfully synthesized and characterized via physico-chemical assessments as sensitizer candidate for solid-state dye sensitized solar cell. Its absorption spectroscopic characteristics have been studied experimentally and theoretically to exhibit mixed $\pi \rightarrow \pi^*$ and $n \rightarrow \pi^*$ transitions. Meanwhile, this dye possesses relatively good HOMO-LUMO gap, 3.06 eV which infers respectable electron charge mobility from amino to ethylene and to NO_2 group. The fabricated DSSC displayed positive response under light intensity exposure although the J_{sc} and PCE value were quite low for photovoltaic measurement. Overall, the findings indicated that

stilbene-based compound can be employed as an ideal sensitizer in optoelectronic devices.

ACKNOWLEDGEMENT

The authors would like to express their gratitude to The World Academy of Sciences (TWAS) for the international research grant (17-016RG/REN/AS_C-FR3240300051), School of Fundamental Science, School of Ocean Engineering and Institute of Marine Biotechnology (IMB) Universiti Malaysia Terengganu for the facilities and research aids.

REFERENCES

1. Joly, D., Pellejà, L., Narbey, S., Oswald, F., Chiron, J., Clifford, J. N., Palomares, E., & Demadrille, R. (2014) A robust organic dye for dye sensitized solar cells based on iodine/iodide electrolytes combining high efficiency and outstanding stability, *Scientific Reports*, **4**, 4033.
2. Mishra, A., Fischer, M. K., & Bäuerle, P. (2009) Metal-free organic dyes for dye-sensitized solar cells: From structure: Property relationships to design rules, *Angewandte Chemie International Edition*, **48**(14), 2474-2499.
3. Liang, M., & Chen, J. (2013) Arylamine organic dyes for dye-sensitized solar cells, *Chemical Society Reviews*, **42**(8), 3453-3488.

4. Seo, K. D., Lee, M. J., Song, H. M., Kang, H. S., & Kim, H. K. (2012) Novel D- π -A system based on zinc porphyrin dyes for dye-sensitized solar cells: synthesis, electrochemical, and photovoltaic properties, *Dyes and Pigments*, **94**(1), 143-149.
5. Yusof, M. S. M., Pazil, A. M., Kadir, M. A., & Yamin, B. M. (2007) N-(3, 4-Dichlorophenyl)-N'-(phenylacetyl) thiourea, *Acta Crystallographica Section E: Structure Reports Online*, **63**(3), o1302-o1303.
6. Khairul, W. M., Daud, A. I., Hanifaah, N. A. M., Arshad, S., Razak, I. A., Zuki, H. M., & Erben, M. F. (2017) Structural study of a novel acetylthiourea derivative and its evaluation as a detector of benzene, *Journal of Molecular Structure*, **1139**, 353-361.
7. Fang, Z., Wu, F., Jiao, Y., Wang, N., Au, C., Cao, C., & Yi, B. (2018) Effects of styrene unit on molecular conformation and spectral properties of CN-PhCH=NPhCH=CHPh-CN, *Journal of Molecular Structure*, **1159**, 147-155.
8. Qin, C., Zhang, W., Wang, Z., Zhou, M., Wang, X., & Chen, G. (2008) Optical properties of stilbene-type dyes containing various terminal donor and acceptor groups, *Optical materials*, **30**(10), 1607-1615.
9. Um, S. I., Kang, Y., & Lee, J. K. (2007) The synthesis and properties of triazine-stilbene fluorescent brighteners containing a mono-phenolic antioxidant, *Dyes and pigments*, **75**(3), 681-686.
10. Lee, J. K., Um, S. I., Kang, Y., & Baek, D. J. (2005) The synthesis and properties of asymmetrically substituted 4, 4'-bis (1, 3, 5-triazin-6-yl) diaminostilbene-2,2'-disulfonic acid derivatives as fluorescent brighteners, *Dyes and Pigments*, **64**(1), 25-30.
11. Hassan, N., Yusoff, H. M., & Shafawati, S. M. T. (2018) Synthesis and Characterization of P-Nitro Stilbene Schiff Base as a Potential Linker in E-DNA, In *Proceedings of the 2018 8th International Conference on Biomedical Engineering and Technology*, **103-107**.
12. Dinakaran, P. M., & Kalainathan, S. (2013) Synthesis, growth, structural, spectral, thermal, chemical etching, linear and nonlinear optical and mechanical studies of an organic single crystal 4-chloro 4-nitrostilbene (CONS): A potential NLO material, *Spectrochimica Acta Part A: Molecular and Biomolecular Spectroscopy*, **111**, 123-130.
13. Teo, K. Y., Tiong, M. H., Wee, H. Y., Jasin, N., Liu, Z. Q., Shiu, M. Y., Tang, J.Y., Tsai, J.K., Rahamathullah, R. Khairul, W. M. & Tay, M. G. (2017) The influence of the push-pull effect and a π -conjugated system in conversion efficiency of bis-chalcone compounds in a dye sensitized solar cell, *Journal of Molecular Structure*, **1143**, 42-48.
14. Siddick, S. Z., Lai, C. W., & Juan, J. C. (2018) An investigation of the dye-sensitized solar cell performance using graphene-titania (TrGO) photoanode with conventional dye and natural green chlorophyll dye, *Materials Science in Semiconductor Processing*, **74**, 267-276.
15. Tan, C. Y., Farhana, N. K., Saidi, N. M., Ramesh, S., & Ramesh, K. (2018) Conductivity, dielectric studies and structural properties of P (VA-co-PE) and its application in dye sensitized solar cell, *Organic Electronics*, **56**, 116-124.
16. Asiri, A. M., Karabacak, M., Kurt, M., & Alamry, K. A. (2011) Synthesis, molecular conformation, vibrational and electronic transition, isometric chemical shift, polarizability and hyperpolarizability analysis of 3-(4-Methoxy-phenyl)-2-(4-nitro-phenyl)-acrylonitrile: a combined experimental and theoretical analysis. *Spectrochimica Acta Part A: Molecular and Biomolecular Spectroscopy*, **82**, 444-455.
17. Tamer, Ö., Avcı, D., & Atalay, Y. (2015) The effects of electronegative substituent atoms on structural, vibrational, electronic and NLO properties of some 4-nitrostilbene derivatives. *Spectrochimica Acta Part A: Molecular and Biomolecular Spectroscopy*, **136**, 644-650.
18. Saravanan, S., Balachandran, V., & Viswanathan, K. (2014) Spectroscopic investigation of 4-nitro-3-(trifluoromethyl) aniline, NBO analysis with 4-nitro-3-(trichloromethyl) aniline and 4-nitro-3-(tribromomethyl) aniline. *Spectrochimica Acta Part A: Molecular and Biomolecular Spectroscopy*, **121**, 685-697.
19. He, D. H., Li, X. W., Yang, C., & Yang, J. (2012) Characterization and optical properties of novel unsymmetrical stilbene-based 1, 3, 4-oxadiazole derivatives, *Spectrochimica Acta Part A: Molecular and Biomolecular Spectroscopy*, **95**, 184-187.
20. Rotta, R., Neto, Á. C., De Lima, D. P., Beatriz, A., & Da Silva, G. V. J. (2010) Configuration of stilbene derivatives by ¹H NMR and theoretical calculation of chemical shifts, *Journal of Molecular Structure*, **975**(1-3), 59-62.

21. Lu, H., & He, D. (2014) Asymmetric 1, 3, 4-oxadiazole derivatives containing naphthalene and stilbene units: Synthesis, optical and electrochemical properties, *Spectrochimica Acta Part A: Molecular and Biomolecular Spectroscopy*, **124**, 91-96.
22. López-Mayorga, B., Sandoval-Chávez, C. I., Carreón-Castro, P., Ugalde-Saldívar, V. M., Cortés-Guzmán, F., López-Cortés, J. G., & Ortega-Alfaro, M. C. (2018) Ferrocene amphiphilic D- π -A dyes: synthesis, redox behavior and determination of band gaps, *New Journal of Chemistry*, **42(8)**, 6101-6113.
23. Costa, J. C., Taveira, R. J., Lima, C. F., Mendes, A., & Santos, L. M. (2016) Optical band gaps of organic semiconductor materials. *Optical Materials*, **58**, 51-60.
24. Rudhziah, S., Ahmad, A., Ahmad, I., & Mohamed, N. S. (2015) Biopolymer electrolytes based on blend of kappa-carrageenan and cellulose derivatives for potential application in dye sensitized solar cell. *Electrochimica Acta*, **175**, 162-168.